JOURNAL OF AGRICULTURAL AND FOOD CHEMISTRY

Conformational Interpretation of Vescalagin and Castalagin Physicochemical Properties

NICOLAS VIVAS,*,† MICHEL LAGUERRE,§ ISABELLE PIANET DE BOISSEL,#
NATHALIE VIVAS DE GAULEJAC,† AND MARIE-FRANÇOISE NONIER†

Tonnellerie Demptos seconded to the CESAMO (Centre d'Etudes Structurales et d'Analyses des Molécules Organiques) - Université Bordeaux I, 351 Cours de la Libération, F-33405 Talence, France; Institut Europeén di Chimie et Biologie (IECB), 2 Rue Robert Escarpit, F-33607 Pessac, France; and CESAMO - Université Bordeaux I, F-33405 Talence, France

Vescalagin and castalagin are two diastereoisomers. The variability of their principal physicochemical properties, compared with their small structural differences, suggests important conformational variations. This study shows, experimentally, that vescalagin has a greater effect on polarity, oxidizability in solution, and thermodegradability than castalagin. Conformational analysis by molecular mechanics demonstrated that vescalagin was more hydrophilic and was more reactive to electrophilic reagents than castalagin. Experimental results were thus explained and demonstrated the distinct behaviors of vescalagin and castalagin. These results were attributed to the C1 position of the two compounds because vescalin and castalin have comparable characteristics. Experimental data were confirmed and interpreted by molecular mechanics. This work represents one of the first attempts to correlate conformation and the properties of phenolic compounds. This step constitutes a predictive method for the pharmacology or chemistry of new compounds.

KEYWORDS: ***Quercus*** **sp.; ellagitannins; molecular mechanics; structures; properties**

INTRODUCTION

About 10% of the dry weight of European oak heartwood (*Quercus robur* L. and *Q. petraea* Liebl.) contains extractible ellagitannins (*1*), consisting of hexahydroxydiphenic acid ester with glucose (*2*). The principal ellagitannins are vescalagin (**1**) and castalagin (**2**) (*3*, *4*). Most of the other known ellagitannins are derived from these two forms (*5*). These molecules are extremely soluble in water (*6*), highly oxidizable (*7*), and astringent (*8*). All of these properties have antioxidant and antiradical effects on these products (*9*), induce a response to various nucleophilic substitutions (*10*), play a role in wood discoloration (*11*, *12*), and influence the quality and efficacy of fining (*13*). They are also involved in defense phenomena against different kinds of agression (*14*).

In many oak-using technologies, these molecules are likely to play a part during different processing and treatment operations. For instance, when the oakwood used for making barrels in a cooperage is being dried and seasoned outside, the action of microorganisms, rain, sun, and air eliminates a portion of the ellagitannins (*15*) through hydrolysis, leaching, and oxidation. When the wood is toasted, an essential barrel-making process (*16*) enabling aromas to develop (*17*), the heat induced by the burning causes further ellagitannin degradation (*16*, *18*). And, finally, in enology, barrels are used to mature and age wines and spirits (*19*, *20*). Thus, during the progressive solubilization of ellagitannins, oxidizing processes slowly transform these molecules into polymerized and colored polyphenols (*21*). They then contribute to the color and the taste of wines and spirits stored in barrels. These same molecules also intervene in the redox reactions, which modify the structure of tannins and the color substances of red wines (*7*).

Although **1** and **2** are isomers with similar structures (*22*), their physical and chemical behaviors are different. First, with reverse phase HPLC, there is a time lag of several minutes in their retention times (*23*); their oxidizability and thermal degradation are very different (Moutounet and Scalbert, personal communication). However, such behavioral differences are uncommon in stereoisomers and, as yet, no explanation has been found for them. The present work proposes, first, to study the polarity of **1** and **2** on an HPTLC plate and their oxidation and thermal degradation kinetics and to suggest a plausible interpretation of their physicochemical characteristics by analyzing their respective conformations. Understanding these differences in behavior should contribute to a better knowledge of a number of reactions involving these two ellagitannins. Acid hydrolysis of **1** and **2** produces ellagic acid (**3**) as well as vescalin (**4**) and castalin (**5**) respectively, for which C1 stereochemistry is preserved. Verifying whether isomerism imparts similar properties to **1**/**4** and **2**/**5** should prove to be of interest.

* Author to whom correspondence should be addressed [telephone +33(0) 5.40.00.25.78; fax +33(0) 5.40.00.26.23; e-mail n.vivas@cesamo.u-bordeau1.fr].
† Tonnellerie Demptos seconded to the CESAMO.
§ Institut Europeén de Chimie et Biologie (IECB).
# CESAMO - Université Bordeaux I.

10.1021/jf030460m CCC: $27.50
Published on Web 03/16/2004

MATERIALS AND METHODS

General Experimental Methods. Details of each experiment are given under Results and Discussion.

Oxidation Experiments. Oxidation of **1**/**2** and **4**/**5** (100 mg·L^{-1}) was realized in triplicate in water [ultrapure water (Mill-Q)] or a hydroalcoholic solution (12% vol ethanol, 5 g·L^{-1} tartaric acid, 1 N NaOH to adjust the pH to 3.5) with 10 mg·L^{-1} iron ($FeSO_4$) and 1 mg·L^{-1} copper ($CuSO_4$). The disappearance of each compound was monitored by HPLC under the conditions described by Scalbert et al. (*23*). The initial oxygen consumption rate was monitored by a Clarck electrode under the conditions described by Vivas et al. (*24*) for oxygen measurements and by Vivas et al. (*25*) for experiment chambers.

TLC Experiments. Migration of each compound was followed by TLC plates (cellulose plates = 10 × 10 × 2 mm of cellulose WF 254 stationary phase and RP18 plates = 10 × 10 × 2 mm of C18 WF 254 stationary phase, Merck). Samples (2 μL of 1 g·L^{-1} aqueous solution for **1**, **2**, **4**, and **5** and aqueous ethanol 50% vol for **3**) were sprayed on plates with a CAMAG automated deposit (automatic TLC sampler III, nitrogen as a propulsion gas; spot dimension = 5 mm). Migration was performed in a horizontal chamber at room temperature (20 °C) with different solvents [solvent I, MeOH/H_2O/HCOOH, 40:50:10, v/v/v; solvent II, MeOH/H_2O/CH_3COOH, 1:89:10; solvent III, aqueous CH_3-COOH (6% vol)]. The plates were then read at 280 nm by a densitometer CAMAG (TLC scanner II) for R_f determination. All equipment was monitored by ATS III software for automated deposits and CATS for the densitometer.

Thermal Experiments. Ten milliliters of aqueous solutions of **1** and **2** (5 g·L^{-1}) was evaporated in a rotary evaporator on a Pyrex tube with a Teflon sealed system. The atmosphere of the tube was then replaced with nitrogen. Tubes were exposed to different temperatures (120, 150, 180, and 200 °C) in duplicate, for 1 h; after cooling residual compounds to 20 °C, we solubilized them in water (10 mL) and analyzed them by reverse phase HPLC (*23*).

Calculation Methods. *Molecular Mechanics.* Calculations were performed on a SGI Indigo platform running MacroModel (*26*) version 5.0 (Columbia University, New York) or Insight II and Discover version 2.3.5 (Biosym Technologies). Conformational minima were found using the modified MM2* (1987 parameters) or MM3* (1991 parameters) force fields as implemented and completed in the MacroModel program. Build structures were minimized to a final RMS gradient of ≤0.005 kJ·Å^{-1}·mol^{-1} via the truncated Newton conjugate gradient (TNCG) method (1000 cycles). Coupling constant calculations were performed using the work of Haasnoot et al. (*27*), as implemented in MacroModel.

Monte Carlo Style Conformational Search. This search is implemented in MacroModel (*28*, *29*). The automatic setup was selected, that is, single bonds variable, chiral centers set, and flexible ring opened. To ensure convergence, 3000 steps were taken per input structure, in an energy range of 15 kJ·mol^{-1} (solution accessible conformation). Each conformer was fully minimized (1000 cycles, TNCG method, RMS ≤ 0.005 kJ·Å^{-1}·mol^{-1}, MM3* force field). The least-used structures were used as starting geometries only if their energies were within the energy window (15 kJ·mol^{-1} of the lowest energy structure yet found). In most cases and particularly with dimers, the extended cutoff option was used (VdW = 8 Å, electrostatic = 20 Å, and H-bond = 4 Å). In these conditions castalagin and vescalagin lead, respectively, to 15 and 19 conformers. In the particular case of castalagin a run was performed with a 50 kJ·mol^{-1} energy range leading to 51 conformers. Following the Monte Carlo search, a cluster analysis was performed with XCluster 1.1 (*30*).

Quantum Mechanics Calculations and Electrostatic Potentials. The MacroModel files were converted into CSSR format using an in-house program, and partial atomic charges were calculated using a CNDO/2 (*31*) method (via modified QCPE no. 274 software). De-orthogonalization was systematically performed. Electrostatic potential maps were calculated using the VSS method via QCPE no. 249 (*32*) software modified so as to use the graphic routines of Biosym Software Technologies program InsightII. The maps were drawn in a 0.5 Å cubic grid.

Molecular Lipophilicity Potential. Fragmental atomic constants were attributed using our own ATTRIFI program (*33*), and the isopotential maps were generated, according to an exponential function (*34*) in a 0.5 Å cubic grid, using our in-house MLP program. For this purpose, the molecule was centered and the grid was built 3 Å further than the outermost atoms. The fragmental atomic constants used were either Broto et al.'s (*35*) or those from our own database. In each case a mean lipophilicity potential was calculated in the space surrounding the molecule.

Table 1. Initial Oxidation Rate of Vescalagin, Castalagin, and Their Respective Acid Hydrolysis Products, Vescalin and Castalin, in Aqueous and Hydroalcoholic Solutions (Experiments Conducted at 25 ± 1 °C in Triplicate)

	V_i[a]	
compound	aqueous solution[b]	hydroalcoholic solution[c]
vescalagin (**1**)	0.32 ± 0.08	0.44 ± 0.09
castalagin (**2**)	0.08 ± 0.02	0.13 ± 0.04
vescalin (**4**)	0.64 ± 0.08	0.78 ± 0.1
castalin (**5**)	0.15 ± 0.08	0.27 ± 0.06
ellagic acid (**3**)	0	0

[a] V_i = initial rate of oxygen consumption (μmol/L/h). Disapperance of compounds was monitored by HPLC analysis. [b] Ultrapure water (Milli-Q). [c] 12% vol ethanol, 5 g/L tartaric acid, 1 N NaOH to pH 3.5, 10 mg/L iron ($FeSO_4$), 1 mg/L copper ($CuSO_4$).

Table 2. R_f of Vescalagin, Castalagin, and Their Respective Acid Hydrolysis Products, Vescalin and Castalin, on Different TLC Plates with Three Solvents (Migrations Were Performed on Horizontal Migration Chamber at 20 ± 1 °C)

TLC conditions[a]	vescalagin (**1**)	castalagin (**2**)	vescalin (**4**)	castalin (**5**)	ellagic acid (**3**)
solvent I					
cellulose	0.64	0.6	nd[b]	nd	nd
RP18	0.92	0.89	nd	nd	nd
solvent II					
cellulose	0.61	0.51	nd	nd	nd
RP18	0.77	0.75	nd	nd	nd
solvent III					
cellulose	0.6	0.53	0.88	0.86	nd
RP18	0.57	0.53	0.78	0.74	nd

[a] Solvent I, MeOH/H_2O/HCOOH, 40:50:10, v/v/v; solvent II, MeOH/H_2O/CH_3COOH, 1:89:10, v/v/v; solvent III, aqueous CH_3COOH (6% vol). Cellulose plate (10 × 10 × 2 mm of cellulose WF 254 stationary phase), RP18 plate (10 × 10 × 2 mm of C18 WF 254 stationary phase). [b] Not determined.

Table 3. Effect of 2 h at Different Temperatures on the Concentrations of Vescalagin and Catalagin (Treatments Were Performed on Sealed Tubes in Dried Nitrogen Atmosphere; Results Are Expessed in Milligrams of Compounds)

	control (t_0)	after 1 h			
compound	20 °C	120 °C	150 °C	180 °C	200 °C
vescalagin (**1**)	50	42	17	0	0
castalagin (**2**)	50	48	26	7	0
ellagic acid (**3**)	50	50	50	48	46

RESULTS AND DISCUSSION

Experimental Analysis of a Few Physicochemical Properties. The polarity of **1** and **2** was evaluated by TLC. Two kinds of fixed phases were used—a normal phase (cellulose) and a reversed phase (C18)—and three kinds of relatively polar solvents. Regardless of the experimental setup, **1** always migrated more than **2** (**Table 2**). In the experimental conditions chosen, it appears that **1** has more polarity than **2**. The loss of

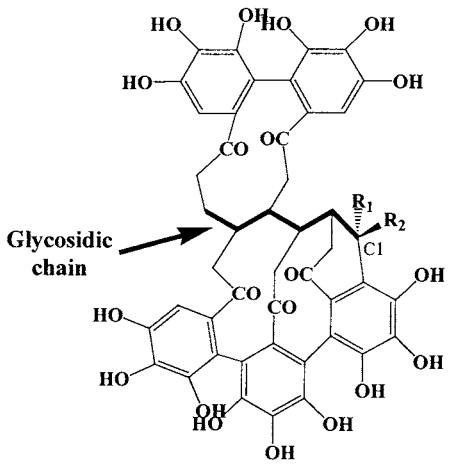

1 vescalagin: R1= H, R2= OH
2 Castalagin: R1= OH, R2= H

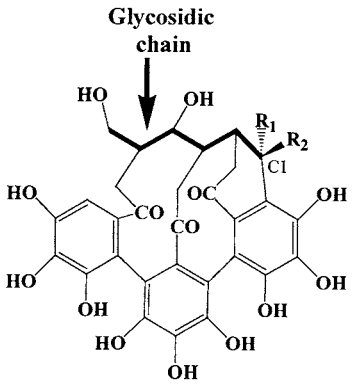

4 vescalin: R1= H, R2= OH
5 castalin: R1= OH, R2= H

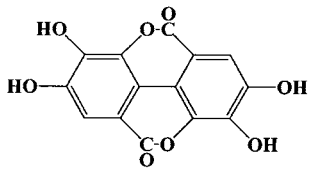

3 ellagic acid

Figure 1. Molecular structures of vescalagin (**1**), castalagin (**2**), vescalin (**3**), castalin (**5**), and ellagic acid (**3**).

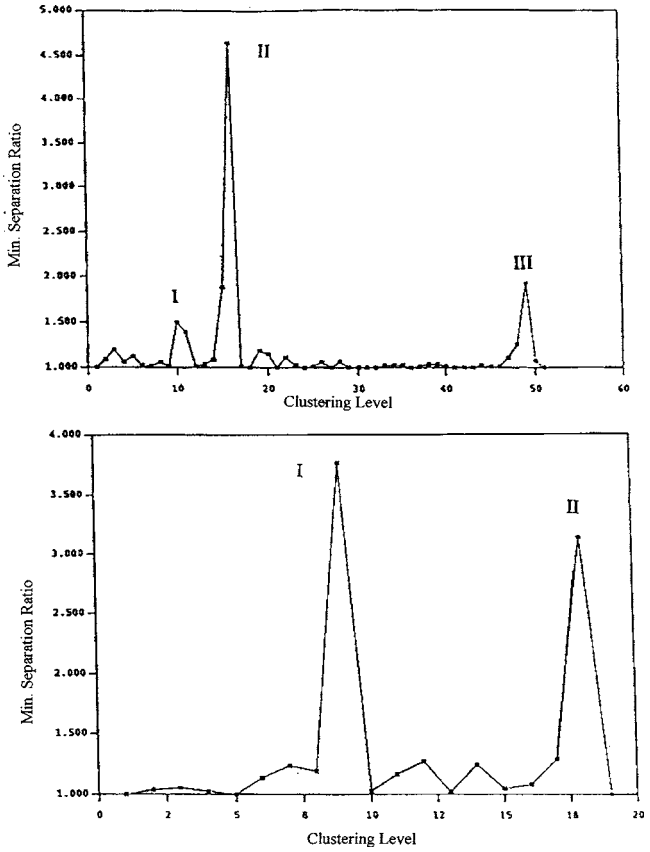

Figure 2. Cluster separation of vescalagin (top) and castalagin (bottom) by RMS technique.

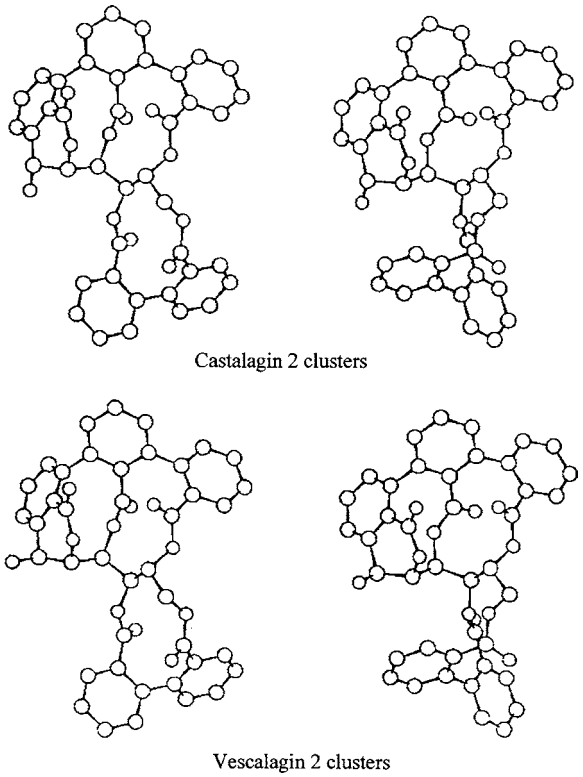

Figure 3. Leader conformers of each cluster family for vescalagin and castalagin.

a hexahydroxydiphenic grouping does not change the order of polarity, which is more favorable for **4** than for **5**. Ellagic acid (**3**), on the other hand, has a very low polarity ($R_f \leq 0.05$).

Monitoring of the initial oxidation rate of the molecules placed in an aqueous solution and in a hydroalcoholic solution shows that **1** and **4** are markedly more oxidizable than **2** and **5** (**Table 1**). In our experimental conditions, **3** was not very oxidizable (V_i in a hydroalcoholic solution = 0.006).

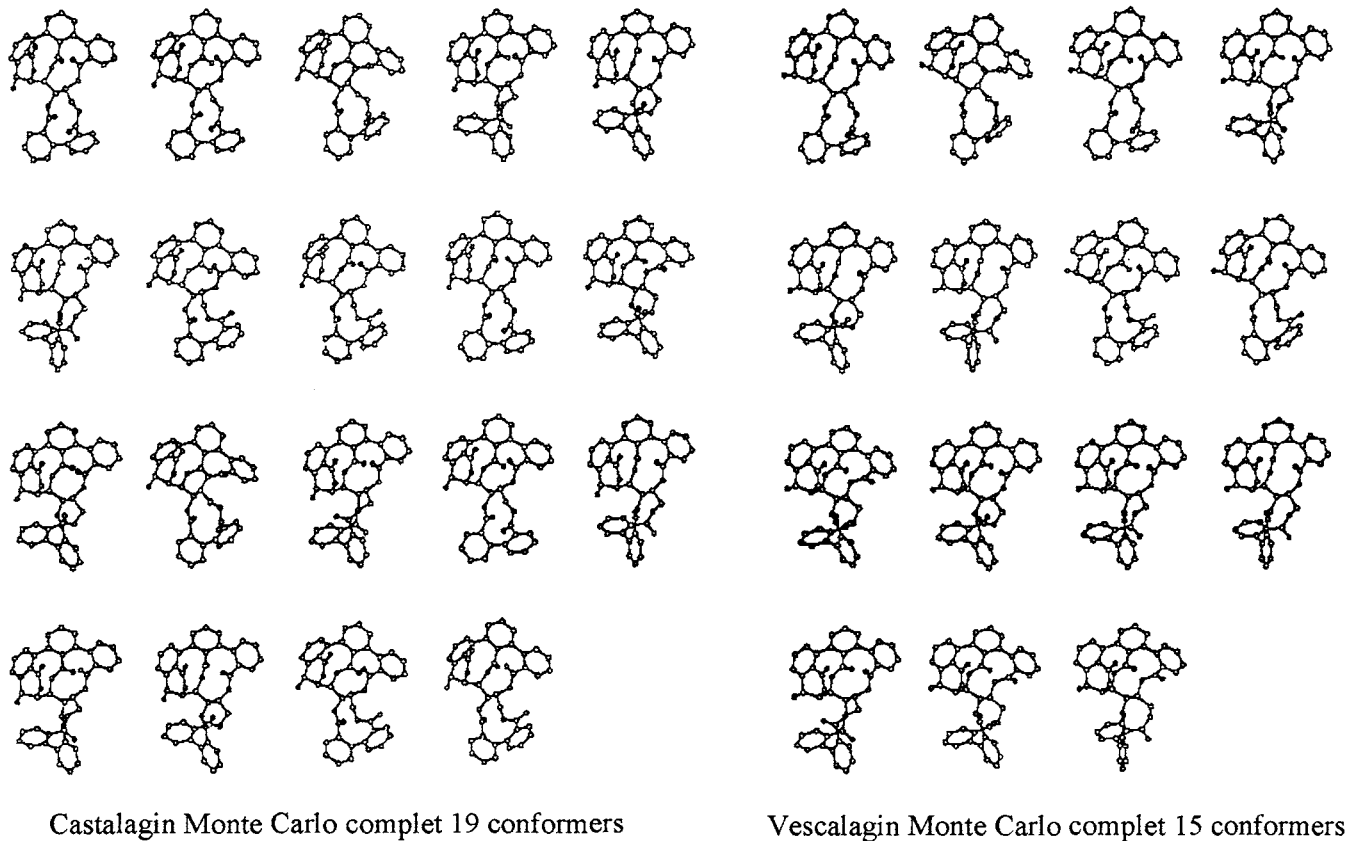

Figure 4. Representation of conformers issued of complete Monte Carlo experiment for vescalagin and castalagin.

Thermal treatment assays showed that **1** is more degraded by heat than **2** (**Table 3**). In identical conditions, **3** does not change significantly.

Analyzing a few physicochemical properties, we noted that **1** is more reactive than **2**. This reactivity expresses itself through greater polarity and higher oxidation and thermal degradation rates. The loss of a hexahydroxydiphenic grouping caused by acid hydrolysis does not modify molecule stereochemistry; thus, **4** produced by **1** remains more reactive than **5** derived from **2**. On the other hand, **3**, released during hydrolysis, turns out to be weakly reactive and relatively apolar. These findings suggest that the physicochemical changes in these two molecules are in fact due to isomerism.

Conformational Analysis of Ellagitannin Monomeres. Our first approach was to check whether the carbon C1 isomerism of glucose was likely to generate a different conformational space. To achieve this, we carried out a complete conformational analysis on two compounds: a Monte Carlo Metropolis search was performed on each conformer found in the previous study. A 15 kJ·mol^{-1} (~3 kcal/mol) energy window was chosen so as to correspond to solution accessible conformations. In these conditions (see Materials and Methods for details) both compounds behaved in a very similar way: **2** and **1** led, respectively, to 15 and 19 different conformers.

Following the Monte Carlo search, a cluster analysis was performed with the Xcluster software program supplied with MacroModel. The conformers obtained can be grouped together in a small number of families that are more representative of the conformational space available to the molecule ("clusters"). The comparison criterion allowing classification is called the critical distance. The critical distance can be the RMS superimposition of the non-hydrogen atoms of the molecules (form criterion) or the RMS of the twisting angles corresponding to the coupling constants ^3J measured in NMR. In this way, all of the possible NMR spectrum families can be defined. With this approach, a conformer can be said to belong to a cluster if it is at less than the critical distance of at least one element of the cluster and at more than this distance than all of the elements of all the other clusters. This implies that a cluster element may very well be further from the critical distance of several elements in the cluster. Moreover, for n conformers, the number of clusterization levels (N) may range from $N = 1$ (tall conformers in a single cluster) to $N = n$ (n clusters with only one conformer). It follows that the cutoff level must be very carefully selected to achieve a really pertinent classification. Selection is facilitated by this criterion of separation because it defines the critical distance ratio between two neighboring clusters: the higher the value, the more pertinent the separation; the closer it comes to 1, the more artificial the separation is (**Figure 1**).

Using the critical distance of the non-hydrogen atom, superimposition RMS makes it possible to extract only two significant conformer families. A study with **1** within a 50 kJ·mol^{-1} window led to a third family (of a total of 51 conformers), but which at best was at 36.8 kJ·mol^{-1} above the minimum energy and was thus normally nonaccessible in solution in normal conditions. The two families found for **2** and **1** (**Figure 2**) are basically identical and correspond in fact to two different conformations of the hexahydroxytriphenic entity connected to carbons C4 and C6; moreover, the population of each family is practically the same. An exhaustive study of all the conformers found showed that the nonahydroxytriphenic group linked to carbons C1, C2, C3, and C5 was particularly rigid and that the hexahydroxytriphenic group linked to carbons C4 and C6 was very mobile (**Figure 3**). The principal cause of such mobility, apart from the smaller number of condensed

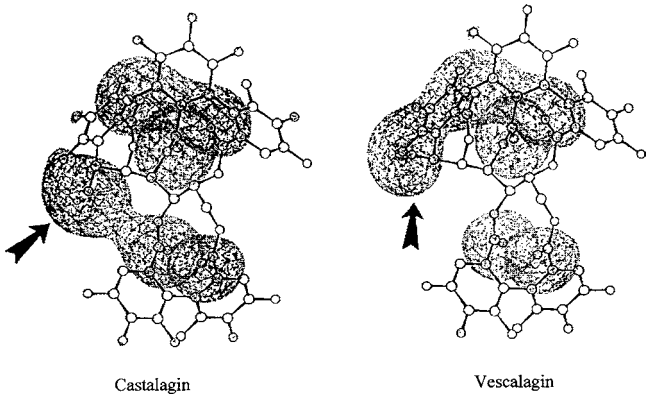

Figure 5. Schematic representation of molecular lipophilicity potential (MLP) volume and repartition for vescalagin and castalagin. Arrow indicates the –OH position in C1.

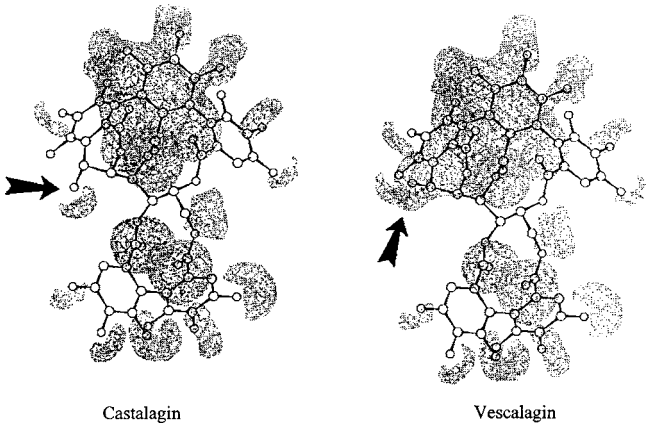

Figure 6. Schematic representation of molecular electrostatic potential (MEP) volume and repartition for vescalagin and castalagin. Arrow indicates the –OH position in C1.

cycles involved, lies in the $C-CH_2-O$ rotation around the carbon C6 of glucose.

Calculated Physicochemical Properties of Ellagitannins. We then attempted to understand how carbon C1 isomerism was able to induce such differences in the properties of the two ellagitannins. On the basis of the conformations defined in the previous section, a certain number of physicochemical properties can be calculated.

Molecular Lipophilicity. Lipophilicity appears to be one of the most accessible properties: TLC or HPLC can provide a measurement indirectly; it can also be calculated empirically through molecular lipophilicity potentials. Using the method described under Materials and Methods, the following orders of magnitude were calculated: Log $P = -3.02$ according to Broto et al. (*35*); there is only one value because this measurement does not take chirality into account. Lipophilic and hydrophilic percentages can be calculated on the solvent accessibility surface. In this case, the same lipophilicity results are obtained: 17.44% for **1** and 17.43% for **2**. On the other hand, the mean lipophilicity potential calculated in the space surrounding the molecule is different: −0.801 for **1** and −0.728 for **2**, which means that **1** absorbs ∼10% more water than **2**; in other words, **1** should be more polar than **2**, which is indeed confirmed experimentally.

Studying the molecular lipophilicity potential maps revealed big differences in hydrophilic distribution between the two ellagitannins (**Figure 4**): the hydrophilic potential of **2** is distributed over two zones of similar volume (one zone around the nonahydroxytriphenic group and one zone around the hexahydroxytriphenic group, also including the two hydroxyls of C1 and of cycle I); with **1**, owing to the OH position in C1, the zone around the hydroxyls of C1 and of cycle I becomes part of the nonahydroxytriphenic zone, which means that there are now two zones with a relation of approximately 1/2. Because **1** has a very large hydrophilic zone, it is probably an energetically unstable form in nonpolar media, unlike **2**, where the two zones are of smaller volume, although the total volume is the same. It is indeed quite possible to imagine that it is the volume of the largest hydrophilic zone, and not the total volume, that determines the overall polarity of the molecule; even if the total hydrophilic volume is identical, it is the partial hydrophilic zone in one piece and with the biggest volume that will be the limiting factor and which will finally define the overall polarity of the molecule.

Electrostatic Potentials and Electronic Properties. The dipole moment was calculated using de-orthogonalized CNDO/2 (*30*); results were as follows: **2** = 2.47 μ and **1** = 3.59 μ (**1** is thus more polarizable than **2**). Using the VSS method (*30*), negative potential extrema were found at −44.39 kcal·mol^{-1} for **2** and at −47.05 kcal·mol^{-1} for **1**; this could mean that **1** is more reactive to electrophilic reagents. Careful examination of electrostatic potential maps reveals interesting differences concentrated around the hydroxyl and the C1: **1** has a vast negative zone surrounding cycles I and II, the gallate ester functions, the two hydroxyls of C1, and the first ortho carbon of cycle I. On the other hand, this same zone in **2** covers neither the external half of cycle I nor the two hydroxyls above; only a small isolated and very excentric zone remains around the dipoles of the C1 hydroxyl (**Figure 5**). The position of the **1** C1 hydroxyl leads to a broad electronic distribution over the whole nonahydroxytriphenic area of the molecule. In the case of **2**, this area is more localized and stops well before the C1 hydroxyl and the first ortho carbon of cycle I. This difference is the most likely explanation for the greater reactivity of **1**.

ABBREVIATIONS USED

HPLC, high-performance liquid chromatography; TLC, thin-layer chromatography; TNCG, truncated Newton conjugate gradient; MM, molecular modeling; RMS, root mean square; VdW, van der Waals; NMR, nuclear magnetic resonance; MLP, molecular lipophilicity potential; MEP, molecular electrostatic potential.

LITERATURE CITED

(1) Scalbert, A.; Monties, B.; Janin, G. Tannins in wood: Comparison of different estimation methods. *J. Agric. Food Chem.* **1989**, *37*, 1324−1329.

(2) Bate-Smith, E. C. Detection and determination of ellagitannins. *Phytochemistry* **1972**, *11*, 1153−1156.

(3) Mayer, W.; Seitz, H.; Jochims, J. C. Uber die gerbstoffe aus dem holz der edelkastanie und deir eich. IV—Die struktur des castalagins. *Liebigs Ann. Chem.* **1969**, *721*, 186−193.

(4) Mayer, W.; Seitz, H.; Jochims, J. C.; Schauerte, K.; Schilling, G. Uber die gerbstoffe aus dem holz der edelkastanie und deir eich. VI—Die struktur des vescalagins. *Liebigs Ann. Chem.* **1971**, *751*, 60−68.

(5) Herve du Penhoat, C. L. M.; Michon, V. M. F.; Peng, S.; Viriot, C.; Scalbert, A.; Gage, D. Structural elucidation of new dimeric ellagitannins from *Quercus robur* L. Roburins A−E. *J. Chem. Soc., Perkin Trans. 1* **1991**, 1653−1660.

(6) Moutounet, M.; Rabier, P.; Puech, J.-L.; Verette, E.; Barrillere, J.-M. Analysis by HPLC of extractable substances in oak wood. Application to a chardonnay wine. *Sci. Aliments* **1989**, *9*, 35−51.

(7) Vivas, N.; Glories, Y. Role of oak wood ellagitannins in the oxidation process of red wines during aging. *Am. J. Enol. Vitic.* **1996**, *47*, 103−107.
(8) Pocock, K. F.; Sefton, M. A.; Williams, P. J. Taste thresholds of phenolic extracts of French and American oak wood: Influence of oak phenols on wine flavor. *Am. J. Enol. Vitic*. **1994**, *45*, 330−334.
(9) Okuda, T.; Yoshida, T.; Hanato, T. Ellagitannins as active constituents of medecinal plants. *Planta Med.* **1989**, *55*, 117−234.
(10) Viriot, C.; Scalbert, A.; Herve du Penhoat, C. L. M.; Moutounet, M. Ellagitannins in woods of sessile oak and sweet chestnut. Dimerization and hydrolysis during wood aging. *Phytochemistry* **1994**, *36*, 1253−1260.
(11) Haluk, J. P.; Schloegel, F.; Metche, M. Chimie de la couleur du bois. Etude comparative des constituants polyphénoliques dans le chêne sain et le chêne coloré. *Holzforschung* **1991**, *45*, 437−444.
(12) Klumpers, J.; Janin, G. Influence of age and annual ring width on the wood colour of oaks. *Holz Roh- Werkst.* **1992**, *50*, 167−171.
(13) Lavisci, P.; Scalbert, A.; Masson, D.; Janin, G. Quality of Turquey oak (*Quercus cerris* L.) wood. I—Soluble and insoluble proanthocyanidins. *Holzforschung* **1991**, *45*, 291−296.
(14) Scalbert, A. Antimicrobial properties of tannins. *Phytochemistry* **1991**, *30*, 3875−3883.
(15) Vivas, N.; Glories, Y.; Doneche, B.; Gueho, E. Observations sur la microflore du bois de chêne (*Quercus sp.*) au cours de son séchage naturel. *Ann. Sci. Nat. (Botanique)* **1991**, *11*, 149−153.
(16) Moutounet, M.; Rabier, P.; Sarni, F.; Scalbert, A. Les tanins du bois de chêne. Les conditions de leur présence dans les vins. *Le bois et la qualité des vins et des eaux-de-vie*; Guimberteau, G., Ed.; Vigne et Vin Publications Internationales: Bordeaux, France, 1992.
(17) Puech, J.-L.; Maga, J. Influence du brûlage du fût sur la composition des substances volatiles et non volatiles d'une eau-de-vie. *Rev. Oenol.* **1993**, *70*, 13−16.
(18) Matricardi, L.; Waterhouse, A. L. Influence of toasting technique on color and ellagitannins of oak wood in barrel making. *Am. J. Enol. Vitic.* **1999**, *50* (4), 519−526.
(19) Vivas, N.; Glories, Y. Les phénomènes d'oxydoréduction liés à l'élevage en barrique des vins rouges: Aspects technologiques. *Rev. Fr. Oenol.* **1993**, *142*, 33−38.
(20) Viriot, C.; Scalbert, A.; Lapierre, C.; Moutounet, M. Ellagitannins and lignins in aging of spirits in oak barrels. *J. Agric. Food Chem.* **1993**, *41*, 1872−1879.
(21) Klumpers, J.; Scalbert, A.; Janin, G. Ellagitannins in European oak wood: Polymerization during wood aging. *Phytochemistry* **1994**, *36*, 1249−1252.
(22) Vivas, N.; Laguerre, M.; Glories, Y.; Bourgeois, G.; Vitry, C. Structure simulation of two ellagitannins from *Quercus robur* L. *Phytochemistry* **1995**, *39*, 1193−1199.
(23) Scalbert, A.; Duval, L.; Peng, S.; Monties, B.; Herve du Penhoat, C. L. M. Polyphenols of *Quercus robur* L. II—Preparative isolation by low-pressure and high-pressure liquid chromatography of heartwood ellagitannins. *J. Chromatogr*. **1990**, *502*, 107−119.
(24) Vivas, N.; Zamora, F.; Glories, Y. Incidence de certains facteurs sur la consommation de l'oxygène et sur le potentiel d'oxydoréduction dans les vins. *J. Int. Sci. Vigne Vin* **1993**, *27*, 23−34.
(25) Vivas, N.; Glories, Y.; Bertrand, A.; Zamora, F. Principe et méthode de mesure du potentiel d'oxydoréduction dans les vins. *Bull. OIV* **1996**, *69*, 617−633.
(26) Mohamadi, F.; Richards, N. G. J.; Guida, W. C.; Liskamp, R.; Lipton, M.; Caufield, C.; Chang, G.; Hendrikson, T.; Still, W. C. *J. Comput. Chem.* **1990**, *11*, 441.
(27) Haasnoot, C. A. G.; De Leeuw, F. A. A. M.; Altona, C. The relationship between proton−proton NMR coupling constants and substituent electronegativities. *Tetrahedron* **1980**, *71*, 2783−2792.
(28) Chang, G.; Guida, W. C.; Still, W. C. An internal coordinate Monte Carlo method for searching conformational space. *J. Am. Chem. Soc.* **1989**, *111*, 4379−4386.
(29) Saunders, M.; Houk, K. N.; Wu, Y. D.; Still, W. C.; Lipton, M.; Chang, G.; Guida, W. C. Conformation of cycloheptadecane. A comparison of methods for conformational searching. *J. Am. Chem. Soc.* **1990**, *112*, 1419−1427.
(30) Shenkin, P. S.; McDonald, D. Q. *J. Comput. Chem.* **1994**, *15*, 899.
(31) Phillips, A. C. *Quantum Chemistry Program Exchange* **1975**, *11*, 274−284.
(32) Giessner-Prettre, C. *Quantum Chemistry Program Exchange* **1974**, *11*, 249.
(33) Croizet, F.; Dubost, J.-P.; Langlois, M.-H.; Audry, E. A fragmental code usable for automatic attribution of lipophilicity atomic constants. *Quant. Struct. Act. Relat.* **1991**, *10*, 211−215.
(34) Fauchère, J.-L.; Quarendon, P.; Kaetterer, L. *J. Mol. Graphics* **1988**, *6*, 203−206.
(35) Broto, P.; Moreau, G.; Vandycke, C. Molecular structures: perception, autocorrelation descriptor and SAR studies. System of atomic contributions for the calculation of the *n*-octanol/water partition coefficients. *Eur. J. Med. Chem.* **1984**, *19*, 71−78.

Received for review June 24, 2003. Revised manuscript received December 18, 2003. Accepted January 20, 2004.

JF030460M